



A High Voltage Gain DC–DC Converter Employing PV Cell and MPPT Technique

Priyamol P¹, Devisree Sasi²

PG Student [PE], Dept. of EEE, Sree Narayana Gurukulam College of Engineering, Kadayiruppu, Kerala, India¹

Assistant Professor, Dept. of EEE, Sree Narayana Gurukulam College of Engineering, Kadayiruppu, Kerala, India²

ABSTRACT: The global demand for electrical power is increasing steadily. The existing energy networks will not be adequate to supply this demand in future. So we have to search for an alternative energy source. Of these the most effective and harmless energy is solar energy. The core of solar power generation system is a solar cell. In this paper a high gain dc-dc converter is used to step up the energy harvested from solar system and MPPT algorithm is used to track the maximum power. The high gain dc-dc converter includes a coupled inductor the leakage inductance of this can be efficiently recycled to the output. A clamping circuit is connected to the primary side of the coupled inductor which clamps the voltage across active switch. The preferred topology has low voltage stress across the switch and can be used for low input and high output voltage applications. A 700 W prototype circuit with 14 V input and 110V output is implemented in the laboratory to verify the performance of the proposed converter.

KEYWORDS: Maximum Power Point Tracking (MPPT), Photo Voltaic module (PV), Coupled inductor, high gain dc-dc converter.

I.INTRODUCTION

Motivation:

As the world energy demand increases and resources begin to wane the search for alternative energy sources has become an important issue. A lot of research has been done in the area of unlimited energy resources such as wind power generation and solar energy transformation. Of these the most effective and harmless energy is solar energy. The use of solar energy instead of fossil fuel combustions particularly in areas of simple applications like low to medium water heating or battery charging can reduce the load of harmful emissions to the environment. The use of solar energy instead of fossil fuel combustions particularly in areas of simple applications like low to medium water heating or battery charging can reduce the load of harmful emissions to the environment. This energy can be harvested by use of photovoltaic (PV) arrays. PV generation plant needs not a specific geographic or geo-morphological requirement such as the wind and micro-small hydropower generation. In contrary, PV generation plant can be built in almost any area where the sun irradiation is available; allows the flexibility to determine the place of the plant according to its main allotment. In addition, the module-based production of PV plant components that enables one to build and adjust the size of PV plant from small capacity and then expand it to follow the High Step Up Boost Converter with MPPT Control. Demand growth is also one of advantages of this type of generation system. All of these facts make the PV modules an interesting choice for the development of electrical energy.

Application:

We can easily classify solar energy according to its basic use, passive solar energy and active solar energy. Passive Solar Energy is a method in which solar energy is harnessed in its direct form without using any mechanical devices. The Active Solar Energy employs mechanical or electrical equipment for functioning and increase system efficiency. As an example water pumps are used to circulate water through the active solar energy water heating system. Use of solar energy is increasing in homes as well. Residential appliances can easily use electricity generated through solar power. On roofs of different buildings we can find glass PV modules or any other kind of solar panel. These panels are used there to supply electricity to different offices or other parts of building in a reliable manner. Another application is solar lighting these lights are also known as day lighting, and work with help of solar power. These lights store natural energy of sun in day time and then convert this energy into electricity to light up in night time. Use of this system is reducing load form local power plants.

International Journal of Advanced Research in Electrical, Electronics and Instrumentation Engineering

(An ISO 3297: 2007 Certified Organization)

Vol. 4, Issue 10, October 2015

Work Summary:

Different types of renewable energy sources have been studied and realized that, the solar energy is the most important and clean one. The concepts of PV cell and its characteristics have been studied. The output voltage generated from the PV generation system is at low level. In order to step up this voltage a high step up dc-dc converter is required. A high voltage gain dc-dc converter has been studied. MPPT algorithm is used to track the maximum power. Among different MPPT algorithm Perturb and Observe algorithm is used here.

II. PV MODEL

A Simplified circuit diagram of a PV cell is shown in figure 1. In this model, there is a current source parallel to a diode. The current source represents light generated current that varies linearly with solar irradiation. This is the simplest and most widely used model as it offers a good compromise between simplicity and accuracy. Figure below shows the single diode model circuit.

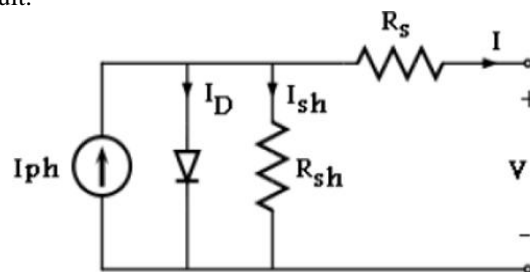


Figure.1 Single Diode model

In this model we consider a current source (I_{ph}) along with a diode and series resistance (R_s). The shunt resistance (R_{sh}) in parallel is very high, has a negligible effect and can be neglected. The output current from the photovoltaic array is

$$I = I_{ph} - I_d \quad (1)$$

$$I_d = I_0 \left[e^{q \left(\frac{V + I R_s}{n k T} \right)} - 1 \right] \quad (2)$$

Where I_0 is the reverse saturation current of the diode, q is the electron charge, V_d is the voltage Across the diode, k is Boltzmann constant (1.38×10^{-19} J/K) and T is the junction temperature in Kelvin (K). From (3.1) & (3.2)

$$I = I_{ph} - I_0 \left[e^{\left(\frac{q V_d}{k T} \right)} - 1 \right] \quad (3)$$

Using suitable approximations

$$I = I_{ph} - I_0 \left[e^{q \left(\frac{V + I R_s}{n k T} \right)} - 1 \right] \quad (4)$$

Where, I is the photovoltaic cell current, V is the PV cell voltage, T is the temperature (in Kelvin) and n is the diode ideality factor.

III. PROPOSED HIGH GAIN DC-DC CONVERTER EMPLOYING PHOTOVOLTAIC CELL AND MPPT TECHNIQUES

Figure 2 shows the circuit diagram of the proposed system. It includes PV cell, dc-dc boost converter with coupled inductor and diode capacitor techniques. The dc-dc converter consist of an active switch Q , an input inductor L_1 , and a coupled inductor, D_1, D_2, D_0 are the diode, C_1 is the storage energy capacitor. The voltage gain can be efficiently increased by using coupled inductor. The secondary winding of the coupled inductor is inserted to a voltage doubler cell, which also increases the voltage gain. The voltage doubler cell consist of regeneration diode D_r , capacitor C_3 . It also consist of a clamp circuit. The clamp circuit consist of diode D_3 and Capacitor C_2 , and is connected to the primary winding of the coupled inductor to clamp the voltage across the active switch to lower voltage level. In the figure $i_{L, K1}$

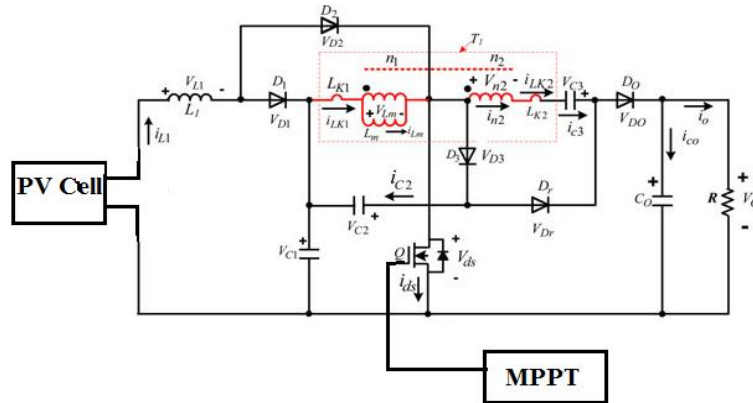


Figure.2 Circuit diagram of proposed converter

and i_{LK2} are the primary and secondary leakage inductance currents. The active switch in the converter is controlled using MPPT algorithm.

Operating Principles Of The Proposed Converter

The figure 2 shows the key waveforms of the proposed converter. The operation can be explained in five modes. The operating stages are described as follows:

Stage 1 [t_0-t_1]

The equivalent circuits of operating stages 1 is shown in fig.4 .At time $t = t_0$, the switch Q is conducting. Diodes $D_1, D_3,$ and D_5 are reverse-biased by $V_{C1}, V_{C1}+V_{C2}$ and $V_O - V_{C1} - V_{C2}$, respectively. Only Diodes D_2 and D_4 are turned ON. The input energy, V_{in} is transferred to the inductor L_1 through D_2 and Q .

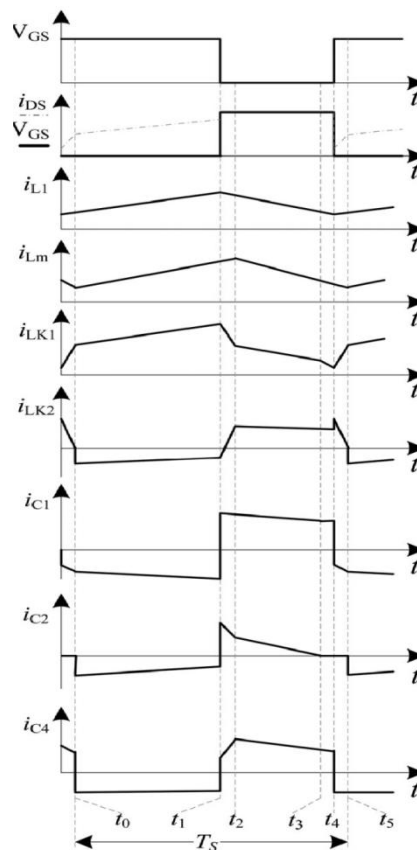


Figure.3. The theoretical waveforms of the proposed converter

International Journal of Advanced Research in Electrical, Electronics and Instrumentation Engineering

(An ISO 3297: 2007 Certified Organization)

Vol. 4, Issue 10, October 2015

Therefore, the current i_{L1} is increasing linearly. The primary voltage of the coupled inductor including magnetizing inductor, L_m and leakage L_{k1} is V_{C1} and the capacitor C_1 is discharging its energy to the magnetizing inductor L_m and primary leakage inductor L_{k1} through Q .

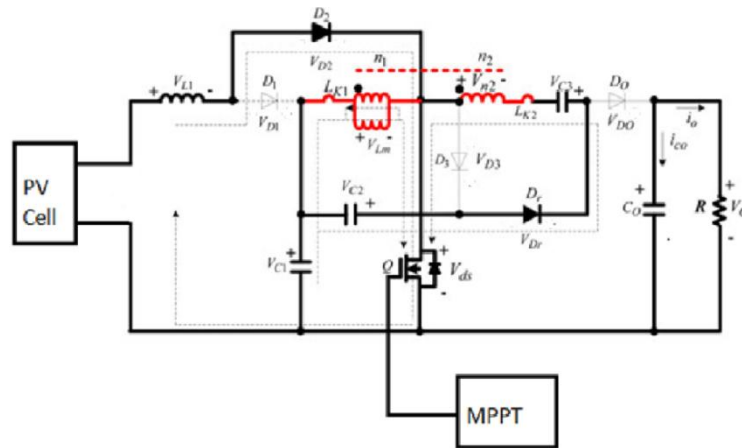


Figure 4. Equivalent circuit of stage 1

Then currents i_{D2} , i_{Lm} , and i_{k1} are increasing. The path of current flow is shown in fig. 4. At the same time, the energy stored in C_2 and C_1 is released to C_3 through D_r . The load 'R' energy is supplied by the output capacitor, C_o . This stage ends at $t = t_1$.

Stage 2 [t_1-t_2]

During this transition interval, Fig. 5 depicts the current-flow path of this stage. At $t = t_1$, the switch Q will get turned off. Then the current through Q is forced to flow through D_3 . At the same time, the energy stored in inductor, L_1 flows through diode D_1 to charge capacitor C_1 instantaneously and the current i_{L1} decreases linearly. Therefore, the diode D_2 is reverse biased by V_{C2} . The diode D_o is still reverse biased by $V_o - V_{C1} - V_{C2}$.

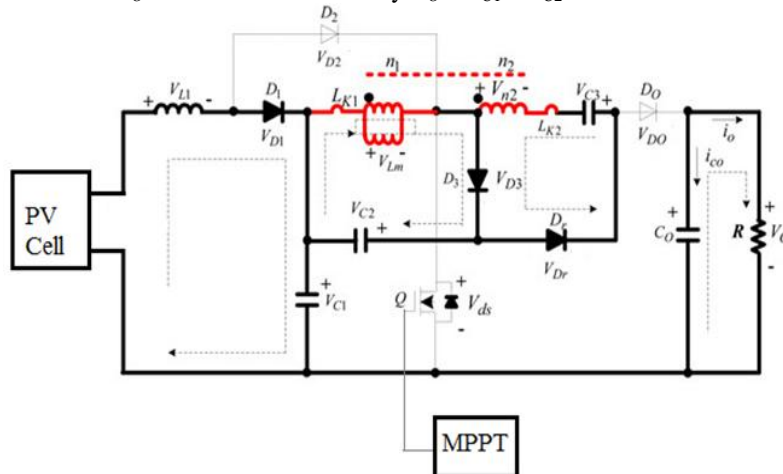


Figure 5. Equivalent circuit of stage 2

Therefore, In this stage, the energy stored in L_{k1} is recycled to C_2 , that is energy stored in inductor L_{k1} flows through diode D_3 to charge capacitor C_2 . The current, i_{Lk2} charging capacitor C_3 , through diode D_3 and regeneration-diode D_r . The voltage stress across Q is the summation of V_{C1} and V_{C2} . The load is supplied by the output capacitors C_o . This stage ends when i_{Lk2} reaches zero at $t = t_2$.

International Journal of Advanced Research in Electrical, Electronics and Instrumentation Engineering

(An ISO 3297: 2007 Certified Organization)

Vol. 4, Issue 10, October 2015

Stage 3 [t_2-t_3]

During this interval, switch Q remains OFF. Since i_{LK2} reaches zero at $t = t_2$, V_{C2} is reflected to the secondary side of coupled inductor T_1 , and thus the regeneration diode, D_3 is blocked by $V_{C3} + NV_{C2}$. At the same time, the diode D_0 starts to conduct. Fig. 6 shows the current-flow path of this stage. The current i_{L1} still decreases linearly, because the inductance L_1 is still releasing its energy to the capacitor C_1 . The energy stored in L_{k1} and L_m is released to C_2 . In this stage, the energy stored in L_m is released to the output through the secondary side of the coupled inductor and C_3 . Thus the leakage inductor energy can be recycled. The voltage stress of the main switch is equal to the summation of V_{C1} and V_{C2} . This stage ends when current $i_{LK1} = i_{LK2}$, thus the current $i_{C2} = 0$ at $t = t_3$.

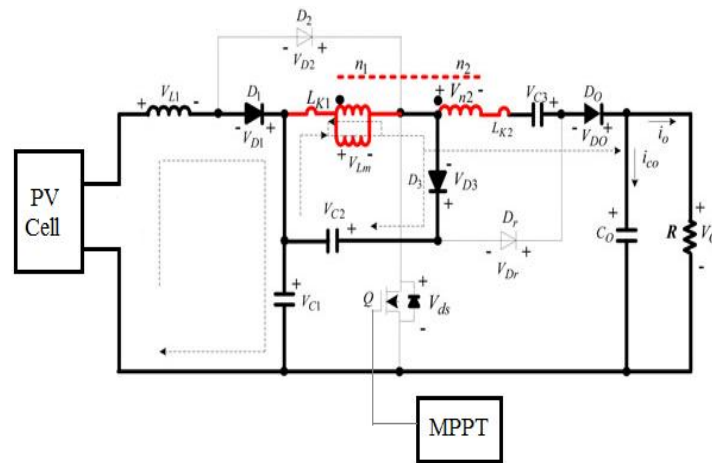


Figure.6 Equivalent circuit of stage 3

Stage 4 [t_3-t_4]

During this time interval, the switch Q , diodes D_2 and D_r is still turned OFF. Since i_{C2} reaches zero at $t = t_3$, the entire current of i_{LK1} flows through D_3 is blocked. The current-flow path of this mode is shown in Fig.7. The energy stored in an inductor L_1 flows through diode D_1 to charge capacitor C_1 continually, so the current i_{L1} is decreasing linearly. The input voltage V_{in} , L_1 , L_m , L_{k1} , the winding n_2 , L_{k2} and V_{C3} are series connected to discharge their energy to capacitor C_0 and load R . At, $t = t_4$ the switch Q become turned on.

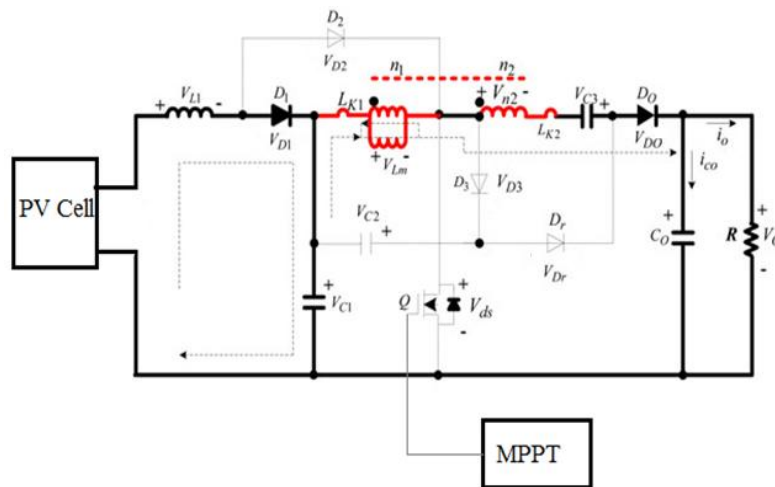


Figure.7 Equivalent circuit of stage 4

Stage 5 [t₄-t₅]

The main switch *Q* is turned ON at *t*₄. During this period, diodes *D*₁, *D*₃, and *D*_r are reverse-biased by *V*_{C1}, *V*_{C1}+*V*_{C2} and *V*_O - *V*_{C1} - *V*_{C2}, respectively. Since the currents *i*_{L1} and *i*_{Lm} are continuous, only diodes *D*₂ and *D*_O are conducting. The current-flow path is shown in Fig.8 . The inductor *L*₁ is charged by input voltage *V*_{in}, and thus the inductor current *i*_{L1} increases almost in a linear way. The blocking voltages *V*_{C1} is applied on magnetizing inductor *L*_m and primary-side leakage *L*_{k1}, so the current *i*_{Lk1} of the coupled inductor is increased rapidly. At the same time, the magnetizing inductor *L*_m keeps on transferring its energy through the secondary winding to the output capacitor *C*_O and load *R*. At the same time, the energy stored in *C*₃ is discharged to the output. Once the increasing *i*_{Lk1} equals the decreasing current *i*_{Lm} and the secondary leakage inductor current *i*_{Lk2} declines to zero at *t* = *t*₅, this stage ends.

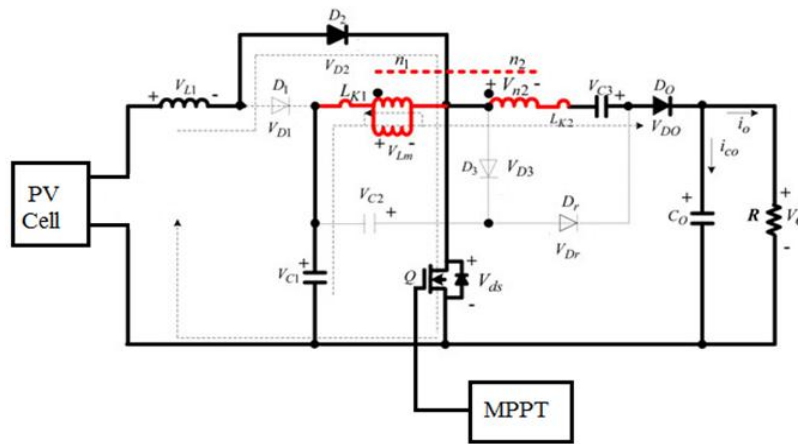


Figure.8 Equivalent circuit of stage 5

IV. DESIGN PROCEDURE

The main equations to design the high voltage dc-dc converter are given below. The input inductor *L*₁ is given by

$$L_1 = \frac{V_{in} D}{\Delta I_{L1} \cdot f_s} \quad (5)$$

Where ‘*V*_{in}’ is the input voltage, ‘*D*’ is the duty ratio, ‘ ΔI_{L1} ’ is the current ripples of inductor current and is equal to 15% of the average input current and ‘*f*_s’ is the switching frequency.

The turns ratio of coupled inductor is given by

$$N = \frac{V_o}{V_{in}} (1 - D)^2 - 2 \quad (6)$$

Where ‘*N*’ is the total number of turns, ‘*V*_o’ is the output Voltage,

The value of capacitors *C*₁, *C*₂, *C*₃, *C*₀ are given by

$$C = \frac{P_{max}}{(V_c \cdot \Delta V_c \cdot f_s)} \quad (7)$$

Where *P* max is the maximum power flowing in the circuit, *V*_c is the voltage across the capacitor and ΔV_c is the maximum tolerant voltage ripple (15% of the *V*_c)

International Journal of Advanced Research in Electrical, Electronics and Instrumentation Engineering

(An ISO 3297: 2007 Certified Organization)

Vol. 4, Issue 10, October 2015

V RESULT AND DISCUSSIONS

A prototype circuit about 40W of the proposed converter is built and tested in the laboratory. The parameters and the component specifications of the proposed converter are described in table I and II.

Prototype Parameters

TABLE I

PARAMETER	PROPOSED CONVERTER
Input Voltage	15-19V(PV MODULE)
Output Voltage	110V
Output Power	40W
Duty Ratio	0.8
Switching Frequency	40KHz

Prototype Components

TABLE II

COMPONENTS	SPECIFICATION
Switch, Q	IRFP250N
Diodes $D_1/D_2/D_3/D_0/D_r$	BYQ28E
Input inductor, L_1	60 μ H
Turns ratio of coupled inductor, N	13/7
Capacitor, C_1	470 μ F/100V
Capacitor, C_2	47 μ F/100
Capacitor, C_3	47 μ F/250V
Capacitor, C_0	470 μ F/600V

The photograph of the proposed converter is shown in figure 9. The prototype circuit uses a PV module BPSX150 providing a maximum power of 30W and a maximum voltage of 19V. The maximum power is tracked by using MPPT technique using Perturb and Observe algorithm. The controller used here is, dsPIC30F2010 which is a 28 pin high performance digital signal controller. It has 6 PWM output channels. By using these channels we can control 6 switches. Here we are using only one switch. The switch used is IRFP250N. The diodes used are BYQ28E which are dual ultrafast soft recovery rectifiers. In order to isolate the circuits opto-couplers TLP250 and IC4N25 are used.

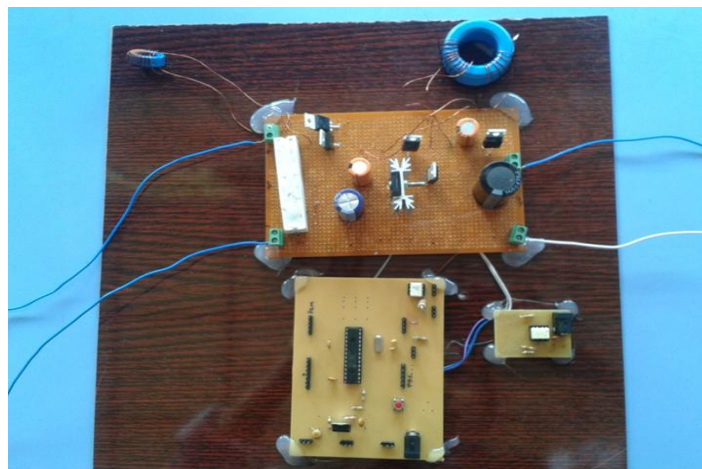


Figure 9 Prototype Of Proposed Converter.

International Journal of Advanced Research in Electrical, Electronics and Instrumentation Engineering

(An ISO 3297: 2007 Certified Organization)

Vol. 4, Issue 10, October 2015

The results obtained with the proposed converter with PV cell and MPPT Technique are presented from Figs. 11 to 13 operating with a resistive load equal to 100 W. The gate signal of the switch, Q is shown in the fig. 10.

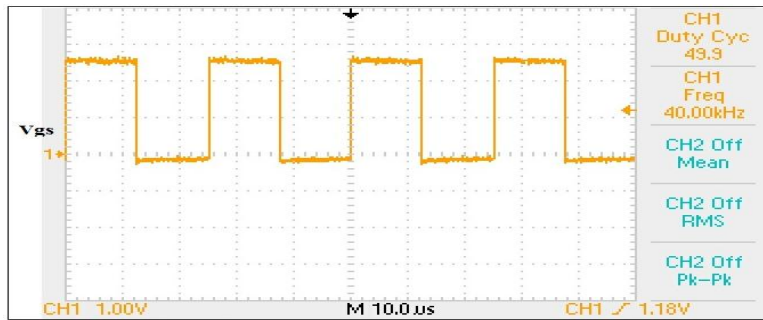


Figure 10 Waveform of switching pulse.

Fig. 11 shows the input voltage and the input current of the modified boost converter employing PV cell and MPPT technique. The input voltage is 14.2V and the input current is 2.37A.

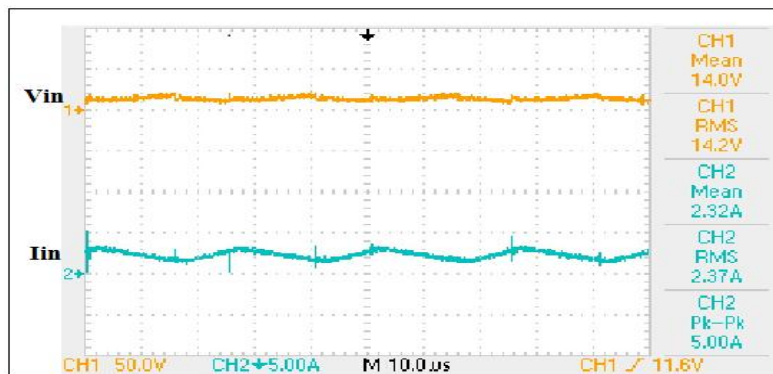


Figure 11 Waveforms of input voltage and input current.

The output voltage and output current is shown in fig. 12 and is equal to 111V, and 351mA respectively. Here the gain is 8. The output power is about 40 W.

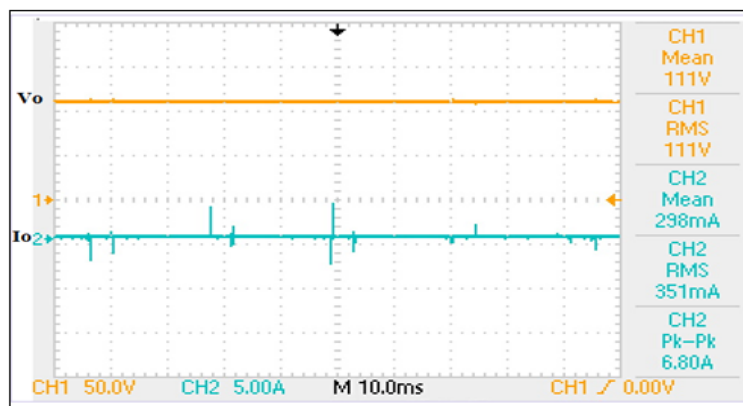


Figure 12 Waveforms of output voltage and output current.

International Journal of Advanced Research in Electrical, Electronics and Instrumentation Engineering

(An ISO 3297: 2007 Certified Organization)

Vol. 4, Issue 10, October 2015

The input inductor current, i_{L1} is presented in Figs.13. It can be seen that the input current is continuous and is optimal for the input current ripple cancellation.

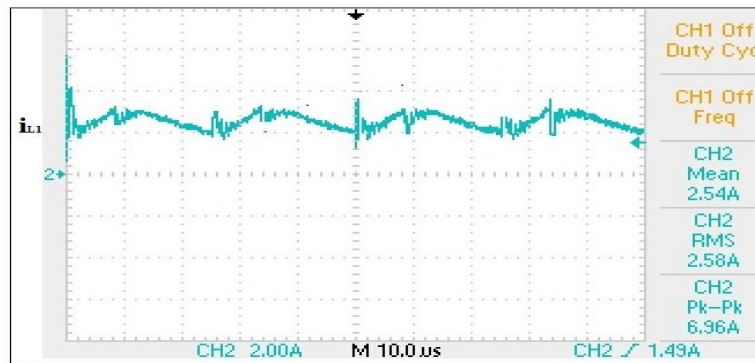


Figure 13 Waveform of inductor current i_{L1} .

The experimental results are similar to the theoretical waveforms presented in Fig. 3.

VI. CONCLUSION AND FUTURE SCOPE

Conclusion

A high gain dc-dc converter using low cost control circuit has been designed for PV system. The converter maintains constant output voltage even though the output voltage from PV system changes. The simulation of the high gain dc-dc converter employing PV Cell and MPPT technique is done using MATLAB Simulink. A prototype of about 40W dc-dc boost converter is constructed and the results are also verified experimentally. The proposed converter uses a coupled inductor, a clamp circuit and a voltage doubler cell. The leakage inductance of the coupled inductor can be efficiently recycled to the output. A clamping circuit is connected to the primary side of the coupled inductor, which reduces the voltage stress across the switch. The switch is controlled by using MPPT technique. A diode capacitor circuit is connected to the secondary side of the coupled inductor, to increase the voltage gain. Here only a single switch is used, this reduces the system complexity and increases the system reliability. The preferred topology can be used for low input and high output voltage applications.

Future Scope

The proposed system can find application in systems with low input and high output voltage. Since the system uses renewable energy source it can be effectively used in wide range of applications, including the ups system.

REFERENCES

1. Xuefeng Hu and Chunying Gong, Member, IEEE, "A High Voltage Gain DC-DC Converter Integrating Coupled-Inductor and Diode-Capacitor Techniques," in *IEEE transactions on Power Electronics*, vol. 29, no. 2, February 2014.
2. Henry S. H. Chung, Member, IEEE, W. C. Chow, S. Y. R. Hui, Senior Member, IEEE, and Stephen T. S. Lee "Development of a Switched-Capacitor DC-DC Converter with Bidirectional Power Flow" *IEEE transactions on Circuits and Systems-i: fundamental theory and applications*, vol. 47, no. 9, September 2000
3. Luiz Henrique Silva ColadoBarreto, ErnaneAntônioAlvez Coelho, Member, IEEE, Valdeir José Farias, João Carlos de Oliveira, Luis Carlos de Freitas, and João Batista Vieira, "A Quasi-Resonant Quadratic Boost Converter Using a Single Resonant Network". *IEEE transactions on Industrial Electronics*, vol. 52, no. 2, April 2005
4. B. Axelrod, Y. Berkovich, and A. Ioinovici, "Switched-capacitor/ switched-inductor structures for getting transformerless hybrid DC-DC PWM converters," *IEEE Trans. Circuits Syst. I*, vol. 55, no. 2, pp. 687–696, Mar. 2008.
5. K. D. Kim, J. G. Kim, Y. C. Jung, and C. Y. Won, "Improved non-isolated high voltage gain boost converter using coupled inductors," in *Proc. IEEE Int. Conf. Electric. Mach. Syst.*, Aug. 2011, pp. 20–23.
6. Y. Deng, Q. Rong, W. Li, Y. Zhao, J. J. Shi, and X. N. He, "Single-switch high step-up converters with built-in transformer voltage multiplier cell," *IEEE Trans. Power Electron.*, vol. 27, no. 8, pp. 3557–3567, Aug. 2012.
7. S. Lee, P. Kim, and S. Choi, "High step-up soft-switched converters using voltage multiplier cells," *IEEE Trans. Power Electron.*, vol. 28, no. 7, pp. 3379–3387, Jul. 2013.
8. G. Spiazzi, P. Mattavelli, J. R. Gazoli, R. Magalhaes, and G. Frattini, "Improved integrated boost-flyback high step-up converter," in *Proc. IEEE Ind. Technol. Conf.*, Mar. 2010, pp. 1169–1174.